



## PRELIMINARY INSIGHTS ON THE INELASTIC SEISMIC RESPONSE OF STRUCTURAL SYSTEMS UNDER PULSE-LIKE GROUND MOTION

C. Demartino<sup>(1)</sup>, G. Quaranta<sup>(2)</sup>, F. Mollaioli<sup>(3)</sup>

<sup>(1)</sup> Assistant Professor, Zhejiang University – University of Illinois at Urbana Champaign Institute, 718 East Haizhou Road, Haining, 314400 Zhejiang, PR China, [cristoforo.demartino@me.com](mailto:cristoforo.demartino@me.com)

<sup>(2)</sup> Associate Professor, Department of Structural and Geotechnical Engineering, Sapienza University of Rome, via Eudossiana 18, 00184 Rome, Italy, [giuseppe.quaranta@uniroma1.it](mailto:giuseppe.quaranta@uniroma1.it)

<sup>(3)</sup> Associate Professor, Department of Structural and Geotechnical Engineering, Sapienza University of Rome, via Gramsci 53, 00197 Rome, Italy, [fabrizio.mollaioli@uniroma1.it](mailto:fabrizio.mollaioli@uniroma1.it)

### **Abstract**

Near-fault pulse-like seismic events exhibit a pulse in the velocity time history that mainly occurs in the strike-normal direction at locations towards which the earthquake rupture has propagated. The large damage potential associated with such seismic events is due to high displacement and velocity demands, together with the transmission of a large amount of energy in a relatively short time. In presence of specific geological conditions, they can also reveal unusual peaks of the spectral values in the long-period range. Additionally, it is well known that the intensity level of the vertical shaking close to the causative fault can be exceptionally high. Within this framework, the present study presents a preliminary sensitivity analysis of the inelastic response of structural systems under near-fault pulse-like ground motion accounting for the vertical component through the P-Delta effect for better understanding the damage potential of such seismic events and for supporting the development of proper design guidelines. First, some seismic records have been selected and processed. The dominant pulse embedded in the selected records and the corresponding pulse period value are derived through a recent methodology based on the Variational Mode Decomposition technique. Several nonlinear dynamic analyses are then performed. Specifically, elastic and inelastic response spectra are first calculated taking into account the whole seismic signal and the dominant pulse only, without and with vertical seismic component and P-Delta effect. In doing so, acceleration, velocity, displacement and energy spectra are carried out and analyzed. The preliminary results here reported indicate that for large fundamental periods of the oscillator (e.g., larger than 3 s) the response can be significantly higher when the vertical component of the accelerogram and P-Delta effect are also taken into account. Moreover, it is found that the nonlinear behavior of the oscillator can have a beneficial or detrimental effect. The outcomes of this preliminary analysis aim at providing useful insights toward a better characterization of the seismic demand in inelastic structural systems subjected to pulse-like seismic events.

*Keywords: inelastic spectra; near-fault pulse-like seismic ground motion; pulse period; variational mode decomposition.*



## 1. Introduction

Near-fault ground motions have significantly different characteristics compared to the ones observed in earthquakes recorded far away from the seismic source [1]. In fact, compared with an ordinary (non-pulse-like) seismic ground motion, a pulse-like motion typically has large velocity amplitudes at medium-to-low frequencies, a higher energy level and a larger ratio of the peak ground velocity to peak ground acceleration. Previous studies about the seismic response of civil structures show that pulse-like earthquakes often induce an extremely high structural seismic demand, see for instance [2]-[6].

Near-fault pulse-like seismic events exhibit a pulse in the velocity time history that mainly occurs in the strike-normal direction at locations towards which the earthquake rupture has propagated. The large damage potential associated with such seismic events is due to high displacement and velocity demands, together with the transmission of a large amount of energy in a relatively short time. In the presence of specific geological conditions, they can also reveal unusual peaks of the spectral values in the long period range.

Ground motions with velocity pulses caused by near-fault directivity have received a great deal of attention from engineers and seismologists because they can cause severe damage to structures. The characterization of near-fault pulse-like earthquakes has been addressed within several studies. For instance, Baker [7] implemented the Wavelet Decomposition Method for the analysis of pulse-like seismic ground motion records. Mukhopadhyay and Gupta [8] have developed an algorithm to extract the pulses based on a repetitive smoothening technique. Amiri and Moghaddam [9] have proposed a modified version of the S-transform for the decomposition of seismic signals to identify the pulse-like part of near-fault velocity records. Chang et al. [10] have identified the dominant impulsive mode from the original record by minimizing the difference between a numerical pulse model and the velocity time history of the seismic ground motion. On the other hand, Mimoglou et al. [11] have illustrated a direct method to estimate the pulse period: according to their approach, the pulse period corresponds to the period value for which the product of velocity and displacement elastic response spectra for 5% damping attains its maximum value. More recently, Quaranta and Mollaioli [12] proposed an approach based on the use of the Variational Mode Decomposition technique for the analysis of pulse-like ground motion.

It is well recognized that the seismic demands can be larger for pulse-like records as compared with ordinary records. In fact, near-fault pulse-like ground motions caused much of the damage in recent major earthquakes (e.g., 1994 Northridge, 1995 Kobe and 1999 Chi-Chi earthquakes). For such seismic loading condition, the response is sensitive to the pulse period value as compared to the fundamental period of the structure, as shown for the first time by Anderson and Bertero [13] when studying the response of steel frames subjected to ground motions recorded during the 1979 Imperial Valley earthquake.

A widespread tool for studying the dynamics of structural systems is based on the use of response spectrum. In this context, pulse-like ground motions have been receiving increased attention because they can lead to rather peculiar types of elastic and inelastic spectra (e.g., [14]). Only a few recent studies have investigated the inelastic response of single-degree-of-freedom (SDOF) oscillators representing structural systems under pulse-like seismic ground motion (e.g., [14]). However, although the higher seismic demand in structural systems under pulse-like ground motions was extensively demonstrated considering the fault-normal horizontal component, little attention has been paid to the effects due to the vertical component. As a matter of fact, strong motion time histories are usually characterized by high vertical peak accelerations and the ratio between the peak ground acceleration in the vertical and horizontal directions (namely, the V/H ratio) is reported to grow with the decrease of the epicentral distance [15]. Large values of the vertical component can amplify the structural damage and increase the P-Delta effect as previously demonstrated in several studies (e.g., [16]-[17]).

Within this framework, the present study presents a preliminary sensitivity analysis of the inelastic response of structural systems under near-fault pulse-like ground motion accounting for the vertical component through the P-Delta effect for better understanding their damage potential and for supporting the development of proper design guidelines. This paper is concerned with the analysis of near-fault pulse-like seismic events



featuring source-to-site distances normally limited to 15 km, although ground motions having pulse-like characteristic are also possible at longer distances when they are generated in distant sedimentary layers or in case of deep earthquakes (1977 Bucarest earthquake), e.g., [18]. Near-fault pulse-like seismic events are only considered because they are usually characterized by very strong vertical shaking.

The present paper is organized as follows. First, some seismic records have been selected and processed. The dominant pulse embedded in the selected records and the corresponding pulse period value are derived through a recent methodology based on the Variational Mode Decomposition technique. Several nonlinear dynamic analyses are then performed. Specifically, elastic and inelastic response spectra are first calculated taking into account the whole seismic signal and the dominant pulse only, without and with the vertical seismic component and P-Delta effect. In doing so, acceleration, velocity, displacement and energy spectra are carried out and analyzed. The outcomes of this preliminary analysis aim at providing useful insights toward a better characterization of the seismic demand in inelastic structural systems subjected to pulse-like seismic events.

## 2. Automatic extraction of the dominant pulse and estimation of the pulse period

The Variational Mode Decomposition (VMD) technique proposed by Dragomiretskiy and Zosso [19] is here employed for processing near-fault pulse-like seismic ground velocity component in the strike-normal direction according to [12]. Some concepts about the VMD technique are provided hereafter whereas more details can be found in [19]. According to the VMD technique, the bandwidth of the mode is determined through the following procedure: i) compute the analytical signal for each mode using the Hilbert transform in such a way to obtain an unilateral frequency spectrum; ii) shift the mode's frequency spectrum to baseband for each mode, by mixing with an exponential tuned to the respective estimated center frequency; iii) estimate the bandwidth using the H1 Gaussian smoothness of the demodulated signal (i.e., squared L2-norm of the gradient). Formally, this leads to the following constrained variational problem:

$$\min_{v_k(t), \omega_k} \left\{ \sum_{k=1}^N \left\| \partial_t \left[ \left( \delta(t) + \frac{j}{\pi t} \right) * v_k(t) \right] e^{-j\omega_k t} \right\|_2^2 \right\}, \quad (1)$$

$$s. t. \quad \sum_{k=1}^N v_k(t) = v(t)$$

where  $v(t)$  is the signal to be decomposed (i.e., the ground motion velocity),  $v_k(t)$  is the  $k$ th mode and  $\omega_k$  the corresponding center pulsation ( $k = 1, \dots, N$ , in which  $N$  is the number of modes),  $\delta(\cdot)$  is the Dirac delta operator and  $*$  is the convolution operator ( $t$  is the time variable). A convenient way to solve this mathematical programming problem is based on the use of Lagrangian multipliers and quadratic penalty term, in such a way to transform the original constrained optimization into an unconstrained one. In doing so, the augmented Lagrangian is:

$$L = \alpha \sum_{k=1}^N \left\| \partial_t \left[ \left( \delta(t) + \frac{j}{\pi t} \right) * v_k(t) \right] e^{-j\omega_k t} \right\|_2^2 + \left\| v(t) - \sum_{k=1}^N v_k(t) \right\|_2^2 + \left\langle \lambda, v(t) - \sum_{k=1}^N v_k(t) \right\rangle, \quad (2)$$

where  $\lambda$  is the Lagrangian multiplier while  $\alpha$  determines the data fidelity. The solution of the problem given in Eq. (1) is thus obtained as the saddle point of the Lagrangian in Eq. (2) through a sequence of iterative sub-optimizations named alternate direction method of multipliers. The procedure is stopped once a suitable convergence criterion is fulfilled. While the above presentation is framed within the time domain, from a computational standpoint the complete final algorithm is more efficiently implemented in the spectral domain.



Previous applications of the VMD have shown that it is able to precisely detect the embedded modes, largely irrespective of their relative amplitudes and how close their frequencies are. Such features are especially important for the analysis of near-fault ground motions since multiple modes characterized by similar amplitudes and frequencies can be embedded into the seismic record.

Once the seismic velocity  $v(t)$  has been decomposed into its modes  $v_k(t)$  (for  $k = 1, \dots, N$ ), they are approximated by means of a suitable numerical pulse-like waveform  $\hat{v}_k(t)$ . Finally, the dominant pulse is selected from the set of  $N$  waveforms  $\hat{v}_k(t)$  in such a way that the corresponding value of the pulse index  $PI_k$  is the maximum among the ones larger than a given threshold. The related value of  $\omega_k$  is thus used to estimate the pulse period of the ground motion velocity record. In the present work, the numerical pulse-like waveform proposed in [20] is considered whereas the pulse index is defined according to [7]. It is understood, however, that any other suitable choice can be implemented to this end.

### 3. Mechanical system

#### 3.1 SDOF mass-spring-dashpot model

Structural systems under earthquake are usually represented by idealization as a SDOF mass-spring-dashpot model with a time-varying applied ground acceleration, see Fig. 1 (left). The equation of motion of a viscous damped single degree of freedom (SDOF) oscillator subjected to ground acceleration is:

$$m\ddot{u}(t) + c\dot{u}(t) + f_S(u(t)) = -m\ddot{u}_g(t), \quad (3)$$

where  $m$  is the mass,  $c$  is the viscous damping coefficient,  $f_S$  is the restoring force (that can be linear or non-linear) depending on the relative displacements of the mass  $u$ ,  $\dot{u}$  and  $\ddot{u}$  are the relative velocity and accelerations of the mass with respect to the ground.

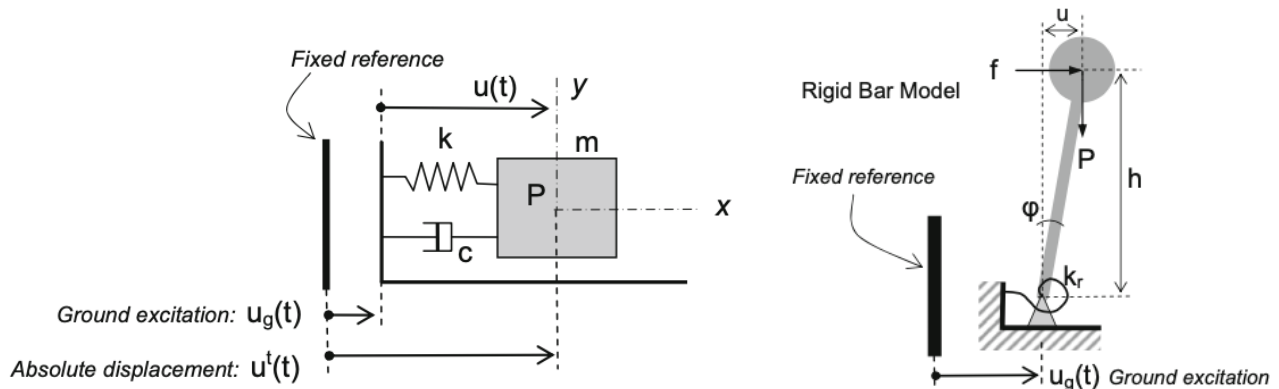


Fig. 1 – SDOF system typically used in earthquake engineering (left) and SDOF model (inverted pendulum) for considering P-Delta effect (right), after [21].

#### 3.2 Inverted pendulum SDOF model accounting for P-Delta effect

In order to account for P-Delta effect, a mass-on-rod type pendulum is used and additional variables are considered for the SDOF system, namely the height of the system  $h$  and the vertical seismic input. This model was widely used in the literature (e.g., [21],[22] and [23]). As shown in Fig. 1 (right), the deformation of the SDOF system is concentrated at the elastoplastic spring located at the base of the rigid column. The term  $P =$



$m\ddot{u}_{g,v}(t)$  is the vertical load equal to the mass multiplied by the vertical component of the ground motion acceleration.

To account for P-Delta effect on the dynamic response, a new term is introduced into the equation of motion, thereby obtaining:

$$m\ddot{u}(t) + c\dot{u}(t) + f_s(u(t)) - \frac{m\ddot{u}_{g,v}(t)}{h}u(t) = -m\ddot{u}_g(t), \quad (4)$$

The additional term of Eq. (2) is a nonlinear geometric stiffness (P-Delta effect).

### 3.3 OpenSees model

To investigate the effects of the pulse-like seismic ground motion characteristics on inverted pendulums with different natural periods, a parametric 2D numerical model was built within the OpenSees framework [24] (Version 3.1.0, 64-bit) and by invoking each analysis using Matlab©.

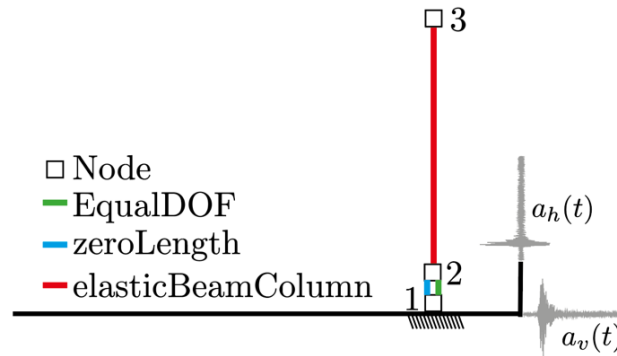


Fig. 2 – OpenSees model

The 2D model herein considered has 3 degrees-of-freedom (DOFs) for each node, see Fig. 2. The model was created using three nodes: the first two nodes are overlapped and located at the base while the third node is located at a distance  $h$ . The first node is fully constrained while the remaining two are free. The third node has a unit mass in the horizontal and vertical translation. The rotational mass of the third node and the all the masses of the first two nodes are assumed equal to zero. Rayleigh damping with modal damping ratios 5% of critical damping in the first mode is considered. The acceleration ground motions in the horizontal and vertical directions were applied at the constrained base node. The gravity acceleration is neglected in this study.

The column is considered rigid and all the deformations are concentrated at the hinge. The length of the beam is equal to 1. The column is modelled by *elasticBeamColumn Element* with very large values of the stiffness. The hinge at the base of the column was modelled using a *zeroLength Element* connecting the first two nodes. Additionally, the two relative translations were blocked by using a multi-point constraint (*EqualDOF*) between the first two nodes.

Two different constitutive laws for the hinge at the base of the column are considered:

- *Elastic Uniaxial Material*;
- *Steel01 Material*.

*Steel01 Material* is a simple bilinear hysteretic model and the motivation of its use relies on the fact that the majority of the simplified approaches to represent a structural system as a SDOF are mainly based on elastoplastic (e.g., a bilinear strength hardening model with post-yield stiffness equal to zero) or bilinear non-degrading hysteretic model.



In both cases, the initial elastic tangent modulus was set to obtain a defined fundamental period,  $T$ , as follows:  $k_r = (2\pi/T)^2$ . For the *Steel01 Material*, a strain-hardening ratio equal to 0.05 is considered and a yield strength equal to:

$$C_y = \frac{F_y}{mg} \rightarrow F_y = mC_y g \quad (5)$$

is assumed, where  $C_y$  is the dimensionless yield strength.

### 3.4 Numerical data and outputs

The numerical model was used to perform several nonlinear dynamic analyses. The following conditions were analyzed.

- Constitutive behavior of the hinge:
  - Elastic;
  - Inelastic ( $C_y = \{0.5, 0.1\}$ ).
- Seismic input:
  - Horizontal component:
    - whole seismic record;
    - dominant pulse only.
  - Types of component:
    - horizontal component only;
    - vertical and horizontal components (the vertical component was always considered as whole record).

The transient analyses were carried out for a total duration of 100 s with a time step equal to 0.001 s. The analyses were performed for the following values of the fundamental period: 0.01 s, from 0.05 s to 3 s with a time step equal to 0.05, from 3.1 s to 10 s with a time step equal to 0.1 s and, finally, from 11 s to 15 s with a time step equal to 1 s.

The following kinematic outputs are provided:

- response acceleration spectrum (maximum absolute response acceleration for each fundamental period);
- response velocity spectrum (maximum relative response velocity for each fundamental period);
- response displacement spectrum (maximum relative response displacement for each fundamental period).

Spectral energy parameters have been also estimated. Uang and Bertero [25] have previously derived the two basic energy equations, namely the absolute and the relative energy equations. The absolute energy input can be expressed as an equivalent absolute velocity as:

$$V_i = \max_t \sqrt{2 \cdot \int_0^t (\ddot{u}(t) + \ddot{u}_g(t)) \dot{u}_g(t) dt} \quad (6)$$

The relative energy input can be expressed as an equivalent relative velocity as:

$$V_{ir} = \max_t \sqrt{-2 \cdot \int_0^t (\ddot{u}_g(t)) \dot{u}(t) dt} \quad (7)$$



### 4. Results and discussions

#### 4.1 Selected ground motion time histories

Several nonlinear dynamic analyses are performed. Two different ground motion time histories were selected for the present preliminary study. They are characterized by the presence of a clear pulse, high values of the moment magnitude, low Joyner-Boore distance as well as mid-large values of peak ground acceleration (PGA) and pulse period  $T_p$ .

Table 1 – Main characteristics of the selected input ground motion time histories

Tag	Moment magnitude	Joyner-Boore distance [km]	Shear velocity in the upper 30m [m/s]	PGA horizontal component [m/s <sup>2</sup> ]	PGA vertical component [m/s <sup>2</sup> ]	Pulse period value [s]
FN002	6.80	3.92	659.60	5.88	12.40	4.31
FN091	7.62	0.32	487.34	5.51	4.77	11.23

The main characteristics of the selected ground motion time histories is provided in Table 1.

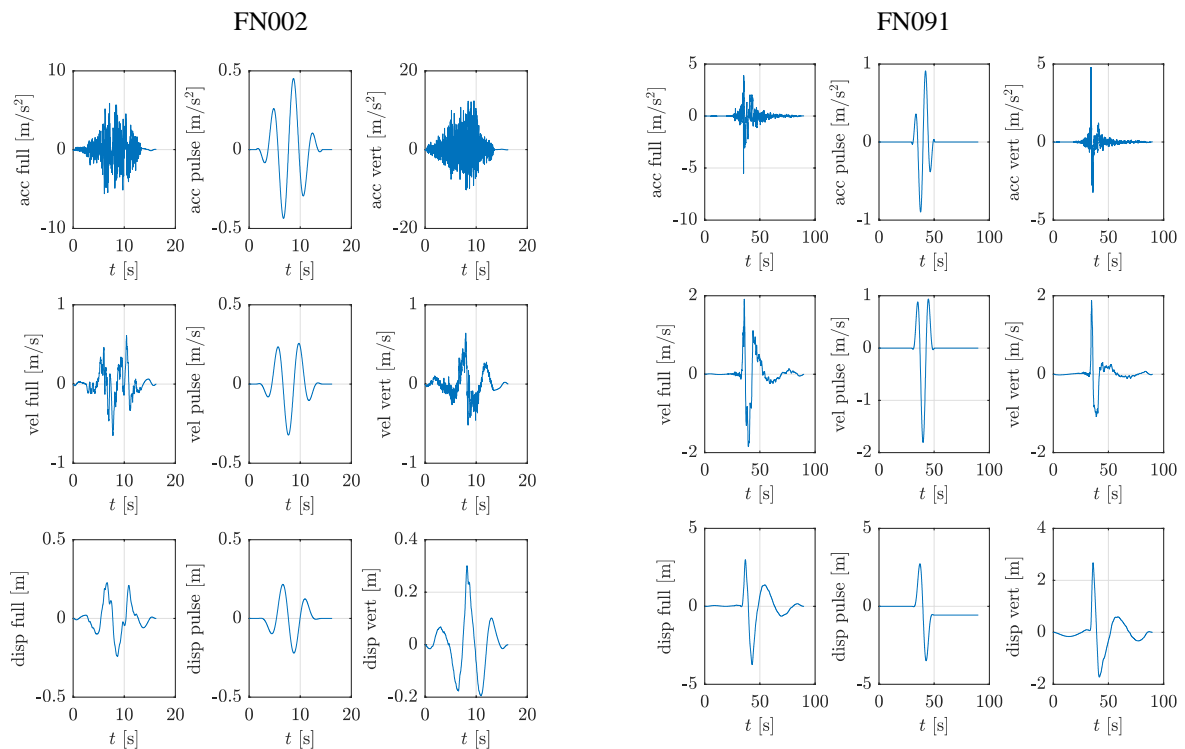


Fig. 3 – Ground motion time histories: acceleration (acc), velocity (vel) and displacement (disp) for full horizontal time history (full), dominant pulse (pulse) and vertical time history (vert)

Ground motion time histories (acceleration, velocity, and displacement) for the full horizontal time history, the dominant pulse only and the vertical time history are reported in Fig. 3. It can be observed in Fig.



3 that both horizontal and vertical components exhibit clear pulse-like velocity and displacement waveforms. In both cases, it can also be noted a good correlation in time of the pulse-like components in the two directions.

#### 4.2 Response spectra

Response spectra in terms of acceleration, velocity, displacement, equivalent absolute velocity and equivalent relative velocity for the two accelerograms previously presented are given from Fig. 4 to Fig. 8. The response spectra are shown considering the full horizontal time history and the dominant pulse, neglecting (continuous line) or considering (dashed line) the vertical time history.

The spectra obtained for the full horizontal time history are typically very sensitive to the variation of  $C_y$  for low values of the fundamental period of the oscillator. On the other hand, the spectra carried out taking into account the dominant pulse only are less sensitive to  $C_y$  (this is more evident when the fundamental period is close to the pulse period). As expected, a general reduction of the spectral values is observed by reducing  $C_y$ , i.e., by increasing the dissipated energy at the base. This difference is more evident for  $C_y = 0.1$ , i.e., when the strength is very low. It should be noted that the PGA is about  $5.5 \text{ m/s}^2$  for both horizontal seismic components, thereby providing a demand for a rigid oscillation in terms of dimensionless yield strength of around  $C_y = 0.5$ .

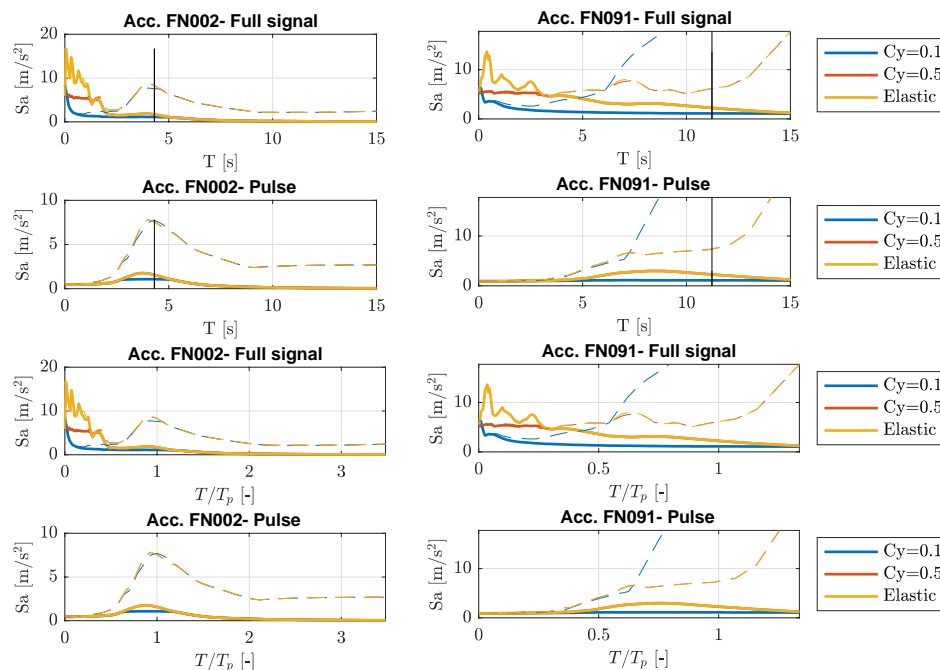


Fig. 4 – Response acceleration spectra for full horizontal time history and dominant pulse, neglecting (continuous line) or considering (dashed line) the vertical time history. The vertical line denotes the dominant pulse  $T_p$ . The first two rows are the spectra as a function of the fundamental period while the last two rows are the spectra as a function of the ratio between fundamental period and pulse period



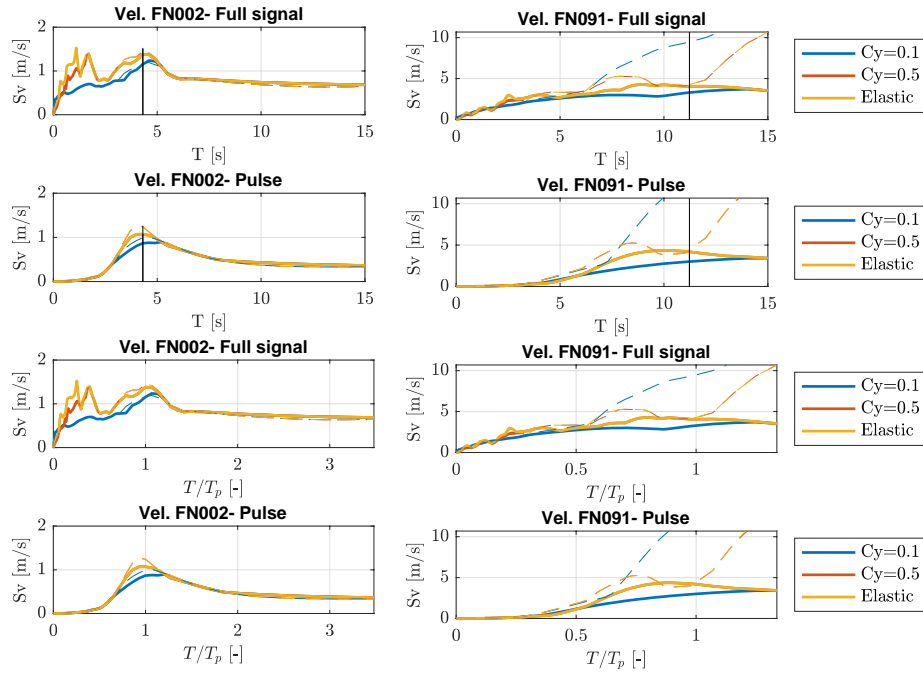


Fig. 5 – Response velocity spectra for full horizontal time history and dominant pulse, neglecting (continuous line) or considering (dashed line) the vertical time history. The vertical line denotes the dominant pulse  $T_p$ . The first two rows are the spectra as a function of the fundamental period while the last two rows are the spectra as a function of the ratio between fundamental period and pulse period

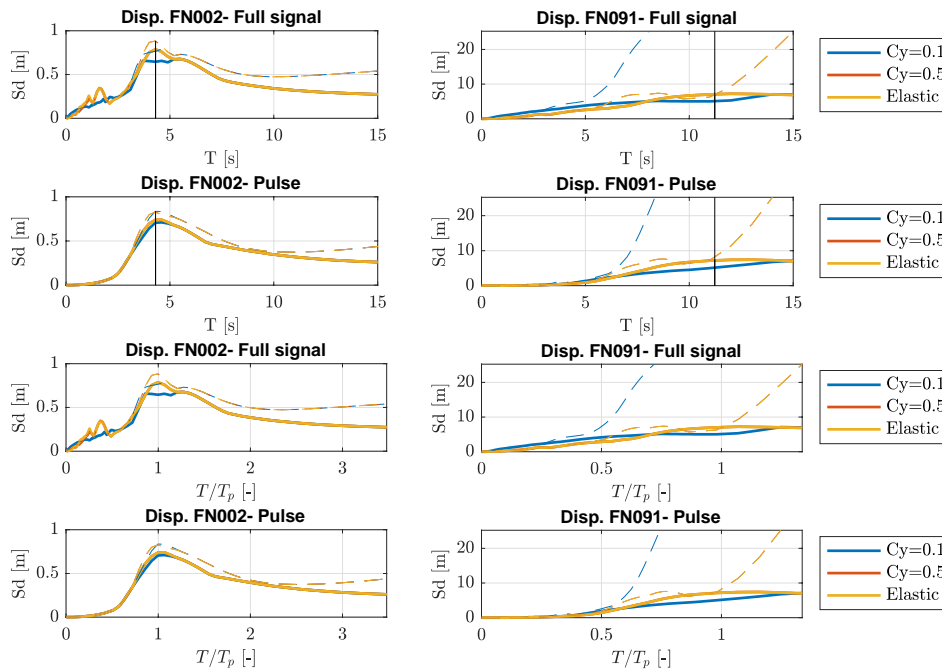


Fig. 6 – Response displacement spectra for full horizontal time history and dominant pulse, neglecting (continuous line) or considering (dashed line) the vertical time history. The vertical line denotes the dominant pulse  $T_p$ . The first two rows are the spectra as a function of the fundamental period while the last two rows are the spectra as a function of the ratio between fundamental period and pulse period

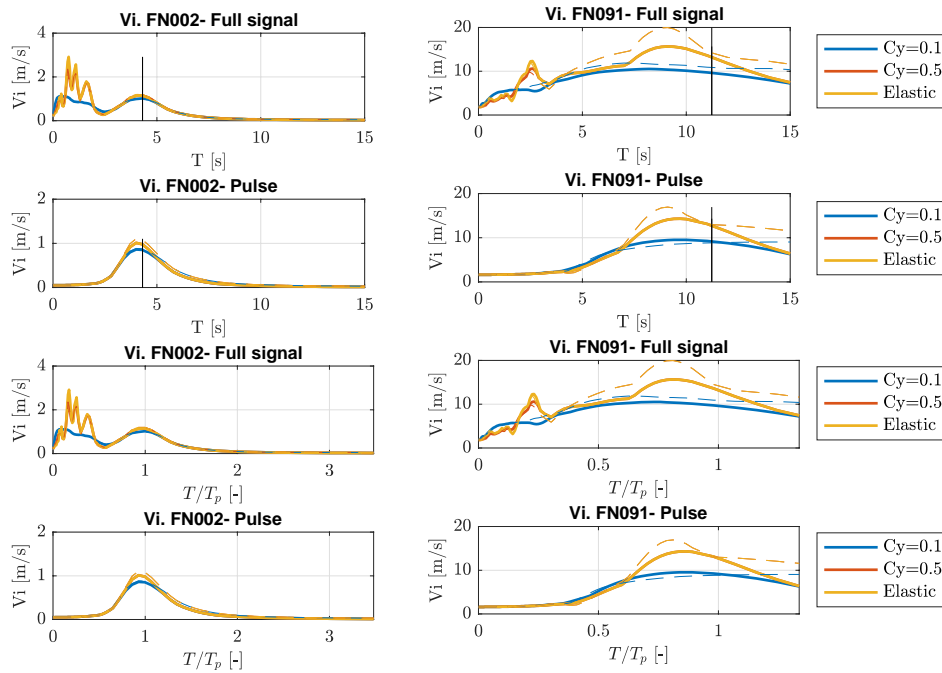


Fig. 7 – Equivalent absolute velocity spectra for full horizontal time history and dominant pulse, neglecting (continuous line) or considering (dashed line) the vertical time history. The vertical line denotes the dominant pulse  $T_p$ . The first two rows are the spectra as a function of the fundamental period while the last two rows are the spectra as a function of the ratio between fundamental period and pulse period

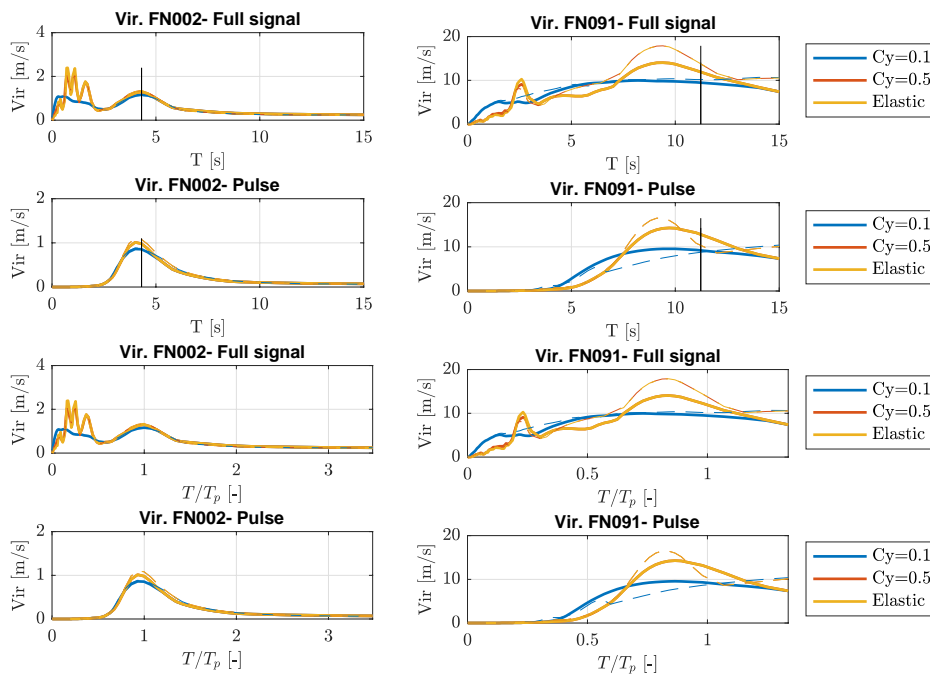


Fig. 8 – Equivalent relative velocity spectra for full horizontal time history and dominant pulse, neglecting (continuous line) or considering (dashed line) the vertical time history. The vertical line denotes the dominant pulse  $T_p$ . The first two rows are the spectra as a function of the fundamental period while the last two rows are the spectra as a function of the ratio between fundamental period and pulse period



For large values of the fundamental period of the oscillator (i.e., for  $T \geq 3$  s), there is a significant difference in the response spectra obtained when neglecting or considering the vertical time history together with the P-Delta effect. Specifically, for the seismic event labelled as FN002, the vertical component has a very large influence on the response acceleration spectrum and, to a lesser extent on velocity and displacement spectra. This is especially evident for fundamental period values close to the pulse period. For the seismic event labelled as FN091, the vertical component affect all response spectra at very high values of the fundamental period of the oscillator. In general, absolute and relative velocities seem less sensitive to the effects due to the vertical component of the seismic ground motion and the nonlinear behavior of the oscillator can have a beneficial or detrimental effect.

## 5. Conclusions

The present study presented a preliminary sensitivity analysis of the inelastic response of structural systems under near-fault pulse-like ground motion accounting for the vertical component through the P-Delta effect. Once selected seismic records have been processed, the dominant pulse and the corresponding pulse period value are derived through a recent methodology based on the Variational Mode Decomposition technique. Several types of elastic and inelastic response spectra are then calculated and discussed taking into account the whole seismic signal and the dominant pulse only, without and with vertical seismic component and P-Delta effect. The results suggest that, for large fundamental period values of the oscillator (i.e.,  $T \geq 3$  s), the response of the oscillation can be quite larger when vertical component and P-Delta effect are taken into account. Moreover, it has been found that the nonlinear behavior of the oscillator can have a beneficial or a detrimental effect.

The outcomes of this preliminary investigation are intended to highlight the key factors toward a better characterization of the seismic demand in inelastic structural systems subjected to pulse-like seismic events. Future work should include the analysis of a large dataset of seismic events, a comprehensive parametric investigation and a refined analysis of the final results in order to develop suitable design recommendations.

## 6. Acknowledgements

The present work is framed within the ReLUIIS 2019–2021 project. The first author acknowledges the Zhejiang University-University of Illinois at Urbana Champaign Institute (ZJUI) for the partial financial support given to the present research.

## 7. References

- [1] Yang F, Wang G, Ding Y (2019): Sensitivity analysis of reinforced concrete frame structures under near-fault pulse-like ground motions using a broadband simulation method. *Journal of Earthquake Engineering*, 1-26.
- [2] Mylonakis G, Voyagaki E (2006): Yielding oscillator subjected to simple pulse waveforms: numerical analysis and closed-form solutions. *Earthquake Engineering and Structural Dynamics*, **35**(15), 1949-1974.
- [3] Mollaioli F, Bruno S, Decanini L, Panza GF (2006): Characterization of the dynamical response of structures to damaging pulse-type near-fault ground motions, *Meccanica* **41**, 23–46.
- [4] Mollaioli F, Bosi A (2012): Wavelet analysis for the characterization of forward-directivity pulse-like ground motions on energy basis, *Meccanica*, (2012) **47**, 203–219.
- [5] Mollaioli F, Liberatore L, Lucchini A (2014): Displacement Damping Modification Factors for pulse-like and ordinary records, *Engineering Structures*, **78**, 17–27.
- [6] Quaranta G, Mollaioli F (2018): On the use of the equivalent linearization for bilinear oscillators under pulse-like ground motion, *Engineering Structures*, **160**, 395-407.
- [7] Baker JW (2007): Quantitative classification of near-fault ground motions using wavelet analysis. *Bulletin of Seismological Society of America*, **97**(5), 486-501.



- [8] Mukhopadhyay S, Gupta VK (2013): Directivity pulses in near-fault ground motions – I: identification, extraction and modeling. *Soil Dynamics and Earthquake Engineering*, **50**, 1-15.
- [9] Amiri GG, Moghaddam SA (2014): Extraction of forward-directivity velocity pulses using S-Transform-based signal decomposition technique. *Bulletin of Earthquake Engineering*, **12**(4), 1583-1614.
- [10] Chang Z, Sun X, Zhai C, Zhao JX, Xie L (2016): An improved energy-based approach for selecting pulse-like ground motions. *Earthquake Engineering and Structural Dynamics*, **45**(14), 2405-2411.
- [11] Mimoglou P, Psycharis IN, Taflampas IM (2017): Determination of the parameters of the directivity pulse embedded in near-fault ground motions and its effect on structural response. *Computational Methods in Earthquake Engineering*. Springer, Cham, 27-48.
- [12] Quaranta G, Mollaioli F (2019): Analysis of near-fault pulse-like seismic signals through Variational Mode Decomposition technique. *Engineering Structures*, 193, 121-135.
- [13] Anderson JC, Bertero VV (1987): Uncertainties in establishing design earthquakes. *Journal of Structural Engineering*, **113**(8), 1709-1724.
- [14] Baltzopoulos G, Vamvatsikos D, Iervolino I (2016): Analytical modelling of near-source pulse-like seismic demand for multi-linear backbone oscillators. *Earthquake Engineering & Structural Dynamics*, **45**(11), 1797-1815.
- [15] Bozorgnia Y, Campbell KW (2004): The vertical-to-horizontal response spectral ratio and tentative procedures for developing simplified V/H and vertical design spectra. *Journal of Earthquake Engineering*, **8**(02), 175-207.
- [16] Demartino C, Vanzi I, Monti G, Sulpizio C (2018): Precast industrial buildings in Southern Europe: loss of support at frictional beam-to-column connections under seismic actions. *Bulletin of Earthquake Engineering*, **16**(1), 259-294.
- [17] Demartino C, Monti G, Vanzi I (2017): Seismic loss-of-support conditions of frictional beam-to-column connections. *Structural Engineering and Mechanics*, **61**(4), 527-538.
- [18] Dai M, Li Y, Liu S, Dong Y (2019): Identification of far-field long-period ground motions using phase derivatives. *Advances in Civil Engineering*, 2019.
- [19] Dragomiretskiy K, Zosso D (2014): Variational mode decomposition. *IEEE Transactions on Signal Processing*, **62**(3), 531-544.
- [20] Mavroeidis GP, Mavroeidis AS (2003): A mathematical representation of near-fault ground motions. *Bulletin of the Seismological Society of America*, **93**(3), 1099-1131, 2003.
- [21] Hernández-Montes E, Aschheim MA, Gil-Martín LM (2015): Energy components in nonlinear dynamic response of SDOF systems. *Nonlinear Dynamics*, 82(1-2), 933-945.
- [22] Semenov ME, Shevlyakova DV, Meleshenko PA (2014): Inverted pendulum under hysteretic control: stability zones and periodic solutions. *Nonlinear Dynamics*, **75**(1-2), 247-256.
- [23] Graizer V, Kalkan E (2008): Response of pendulums to complex input ground motion. *Soil Dynamics and Earthquake Engineering*, **28**(8), 621-631.
- [24] McKenna F (2011): OpenSees: a framework for earthquake engineering simulation. *Computing in Science & Engineering*, **13**(4), 58-66.
- [25] Uang CM, Bertero VV (1990): Evaluation of seismic energy in structures. *Earthquake Engineering & Structural Dynamics*, **19**(1), 77-90.